

## Utilization of Different Additives in Improving Sandy Soil against Liquefaction

*Ahmed Elzamel*<sup>1)</sup>\*, *Ayman Altahrany*<sup>2)</sup> and *Mahmoud Elmeligy*<sup>3)</sup>

<sup>1)</sup> Demonstrator, Structural Engineering Department, Mansoura University, Mansoura, Egypt.

\* Corresponding Author, E-Mail: [ahmedelzamel@mans.edu.eg](mailto:ahmedelzamel@mans.edu.eg)

<sup>2)</sup> Associate Professor, Structural Engineering Department, Mansoura University, Mansoura, Egypt. E-Mail: [atahrany@hotmail.com](mailto:atahrany@hotmail.com)

<sup>3)</sup> Professor of Geotechnical Engineering, Structural Engineering Department, Mansoura University Mansoura, Egypt. E-Mail: [eggroupp\\_Egypt@yahoo.com](mailto:eggroupp_Egypt@yahoo.com)

### ABSTRACT

One of the main risks in low-densified sandy soils with the presence of water and an external force such as an earthquake is the generation of liquefaction. The influence of several types of reinforcement on liquefaction resistance, such as polypropylene fibers, geofibers, cement and polypropylene fibers with cement is shown in this study. Cyclic stress-controlled triaxial tests and cyclic strain-controlled triaxial tests were performed on saturated samples with and without reinforcements under undrained conditions. Cemented specimens were prepared with cement contents ranging from 0% to 3% by weight of dry sand and then cured for 3 days. The lengths of polypropylene fibers are 10 mm and 20 mm, respectively. The fibers were mixed with dry sand-cement mixes containing 0.50% and 1.00% by weight, respectively. Geofiber specimens were prepared in various arrangements. It was found that the liquefaction improvement factor (LIF) increased when fiber content and fiber length increased. The addition of geofibers increased the liquefaction resistance, as the number of layers increased. The addition of 3%C+1%F provided the best liquefaction resistance in this study compared with other additives. Finally, the reinforcement with cement and fibers is crucial for liquefaction resistance of bitumen mastic should be considered beside the asphalt mixture performance and the bitumen rheological behavior.

**KEYWORDS:** Liquefaction, Shear modulus, Cyclic stress, Geofiber, Polypropylene fiber.

### INTRODUCTION

One of the most important earthquake-related processes is liquefaction, which diminishes the resistance of saturated soils. To meet the demands of geotechnical engineering, stabilization techniques have been widely used to increase the strength characteristics of sand. The principal processes of liquefaction in a loose sand deposit during earthquakes are the creation of increased pore water pressure and a drop in mean effective stress (Ishihara, 1993). In soil reinforcement laboratory testing, geotextiles, geofibers, fibers, rubber and cement are most commonly used (Naeini and Zakiyeh, 2014; Kumar et al., 2021).

The cyclic resistance of strengthened specimens

towards liquefaction capability improved, because the number of geotextile layers increased. When the geotextile layer was located close to the pinnacle of the specimen, the liquefaction resistance improved (load application part) (Alibolandi and Moayed, 2015). Mittal and Shukla (2020) discussed how geofiber reinforcement affects the strength of weak subgrade soil. Heavy compaction and soaking CBR tests are performed after the geofibers are put in single and double layers from the top of the mold. Geofiber reinforcement is found to dramatically boost the CBR value, resulting in significant reductions in pavement thickness and cost. The addition of fibers enhanced the sand's shear modulus and reduced the liquefaction phenomenon. When discrete fibers are mixed with the soil, shear strength is improved and post-peak strength loss is minimized (Tang et al., 2007). The effects of fiber

---

Received on 29/4/2022.

Accepted for Publication on 12/9/2022.

content, relative density and confining pressure on loose and medium-dense sand reinforced with polypropylene fibers were evaluated using cyclic triaxial testing. As the fiber content and fiber length increased, the number of loading cycles resulting in liquefaction increased. The improvement in liquefaction resistance was 220 % at a relative density ( $D_r$ ) of 40%, a fiber length of 18 mm and a CSR of 0.25 (Noorzad and Fardad Amini, 2014). Ghadr et al. (2020) utilized undrained cyclic triaxial shear experiments to investigate the effect of fibers on silty sand soil. Increasing fiber content results in an increase in the average number of contacts per particle, dilatation, easier dissipation of excess pore water pressure and lower contact forces thereby improving liquefaction resistance. Robinson et al. (2019) tested HST 95 sand with synthetic fibers in a Cyclic Simple Shear (CSS) programme. The findings showed that adding fibers to the soil prevents major deformations from occurring after the soil has liquefied. Ahmad et al. (2010) conducted drained and undrained triaxial tests on specimens reinforced with 0.25 % and 0.5 % content of different-length fibers (i.e., 15 mm, 30 mm and 45 mm). In addition, the effect of coating on reinforcement was investigated using fibers coated with acrylic butadiene styrene thermoplastic material. Under undrained loading circumstances, reinforced silty sand containing 0.5 % coated fibers of 30 mm length possessed a 25 % increase in friction angle and a 35% increase in cohesiveness compared to unreinforced silty sand. Drained triaxial tests have been conducted on cemented sand specimens strengthened with randomly polypropylene fibers and cement concentrations ranging from 0% to 10% by weight of dry sand beneath cyclic triaxial conditions. Sand stiffness, peak strength and brittleness are all stepped forward through cement (Consoli et al., 2009). Cement and fiber insertions have a large effect at the stress–dilatancy behavior of sand. Shear modulus increased as fiber content increased (F.C. = 0, 0.5 and 1%). The ideal fiber content is demonstrated to be variable and is influenced by the deviator stress ratio (Mirmohammad Sadeghi and Hassan Beigi, 2014). Alhassani (2021) studied the combination of cement kiln dust (CKD) and natural palm fibers to improve the mechanical properties of sandy soil. The results revealed that adding fiber to the soil enhances shear strength significantly up to roughly 1% fiber content, after which the rate of improvement decreases.

Liquefaction resistance, undrained shear strength and stiffness are all improved when polymer fibers and cement are added to silty and clean Toyoura sand. The inclusion of 0 - 2% fibers improves the situation only slightly. In proportion to the percentage added, cement increases the stiffness and liquefaction resistance of the soil (Safdar et al., 2020).

The main goal of this research is to use cyclic stress-controlled triaxial testing and cyclic strain-controlled triaxial testing to assess the liquefaction resistance and shear modulus of the additives. The additives include geofibers, polypropylene fibers, cement and cement with randomly polypropylene fibers. Finally, a comparison between different types of additives is presented.

## MATERIALS AND METHODS

### Test Materials

The properties of the sand used in this study are presented in Table 1. The grain-size distribution curve for sand is shown in Figure 1. The sand is classified as poorly graded sand (SP).

**Table 1. The properties of the sand used in this study**

Property	Value
Soil type	SP
Specific Gravity	2.69
Uniformity coefficient ( $C_u$ )	1.75
Curvature coefficient ( $C_c$ )	0.87
$D_{10}$ (mm)	0.15
Maximum void ratio ( $e_{max}$ )	0.977
Minimum void ratio ( $e_{min}$ )	0.728

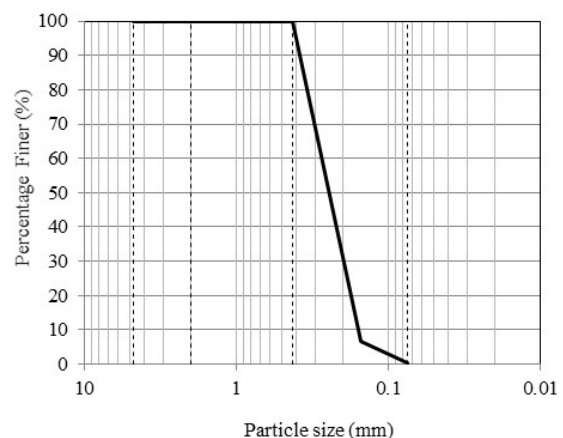


**Figure (1): Grain-size distribution for sand**

Polypropylene fibers were utilized in this study as soil reinforcement, as shown in Figure 2. Polypropylene fibers were with a diameter of 0.018mm, lengths of 10 and 20mm and a specific gravity of 0.91. Fiber contents in reinforced specimens were 0.0, 0.5 and 1 % by weight of dry soil.

For geofiber specimens, as each sand layer was created, the 6.5 cm diameter geofiber inclusions are put horizontally in the specimens. The density of geofibers is 520 gm/m<sup>2</sup>, with a thickness of 2.10mm and a tensile strength of 13.20 kN/m'. Figure 3 depicts geofibers used in this work. Cement contents used in this study were ranging from 0% to 3% by the weight of dry soil. The cement type is ordinary Portland cement (CEM I 42.5 N).



Figure (2): Photograph of the fibers used in this study



Figure (3): Photograph of the geofibers used in this study

### Test Equipment

A tri-axial device that can conduct static and dynamic tensile and compressive load tests in the threshold and alternating load range was used for all of the stress-controlled cyclic triaxial tests as well as strain-controlled cyclic triaxial tests. In this apparatus, cylindrical specimens measuring 70 mm in diameter and 140 mm in height were tested. Figure 4 shows a photo of an experimental setup for reinforced specimen. Figure 5 depicts an overview of the device. The

following things make up the primary system components: load frame and actuator, triaxial cell, air/water bladder and pressure-controlling APC to convert a regulated pressure into a practical pressure range up to 9 bar from a pneumatic pressure supply of up to 10 bar.

A sinusoidal loading frequency of up to 5 Hz is provided by the cyclic triaxial equipment. A displacement transducer with a travel distance of 50 mm and a precision of 0.01 mm was used to measure axial displacement. A load cell with a capacity of 10 kN and a precision of 1 N was used to detect axial load at a periodic time of 0.005 seconds. The electronic volume-measuring device works according to the differential pressure concept and is designed for monitoring minor changes in liquid volume at a high base pressure of up to 10 bar. During testing, an air/water bladder was employed to maintain cell pressure.



Figure (4): Photo of an experimental setup for reinforced specimen



Figure (5): An overall view of the cyclic triaxial system

### Specimen Preparation

In this study, the specimens were prepared by moist tamping. This technique has the benefit of enabling the preparation of any specimen with a wide variety of void ratios (Ishihara, 1993). The under-compaction technique is used to obtain homogeneous specimens (R. S. Ladd, 1978). The two procedures in the phase of preparation are mixing and fabrication. For the mixing process, the required amounts of oven-dried sand, cement and water were combined. The mix had a water content of around 10%. Water is necessary to mix the fibers with the sand and prevent them from floating. The fibers are mixed with cement and sand using an electric mixer. In order to build the specimens, the mixture was divided into five equal portions. These portions were then individually put into a split mold that had a 70-mm diameter and a 140-mm height and each of them was compacted with a metal rod until the appropriate height was reached. Before applying the next layer, the top of each layer was slightly scraped to aid in proper bonding. To achieve the desired relative density of 30%, the specimens were produced in five layers. For the geofiber addition, as each sand layer is created, the 6.5-cm diameter geofiber inclusions are put horizontally in the specimens. Figure 6 shows the different arrangements of geofibers used in this study.

### Test Procedure

A series of cyclic stress-controlled tests as well as cyclic strain-controlled tests were carried out in this study using (ASTM D5311/D5311M-13, 2013) and

(ASTM D3999/D3999M- 11, 2013). Table 2 summarizes the important features of the series of the tests performed in this study. The specimens were prepared and then, a vacuum of 5 kPa was applied to the specimen to achieve the required stability and the mold was dismantled for the non-cement specimens. After the triaxial cell was built and filled with water, the cell pressure was adjusted to 50 kPa and then, distilled de-aired water was passed through the specimen at a pressure of 20 kPa to remove air bubbles in the specimen pores. Back pressure was used to achieve full saturation. At an effective confining pressure of 100 kPa, the specimens were isotopically consolidated. After the consolidation phase was finished, stress-controlled testing was performed under undrained conditions. Axial loads, vertical displacements and pore water pressures were measured at intervals of 0.005 second for the applied sinusoidal waveform with a frequency of 1.0 Hz.

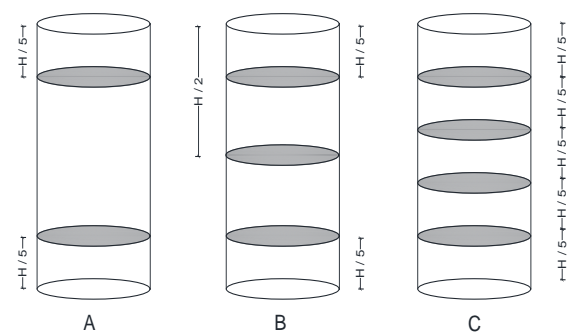


Figure (6): Different arrangements of geofibers

Table 2. Summary of the main series features of tests performed during the current study (CP = 100 kPa and  $D_r = 30\%$ )

	Test type	Additives	FC (%)	CC (%)	FL	Curing period
1	Cyclic stress	Sand	-	-	-	-
2	Cyclic stress	PF	1.0	-	10	-
3	Cyclic stress	PF	1.0	-	20	-
4	Cyclic stress	PF	0.50	-	20	-
5	Cyclic stress	C	-	1.0	-	3days
6	Cyclic stress	C	-	2.0	-	3days
7	Cyclic stress	C	-	3.0	-	3days
8	Cyclic stress	PF+C	1.0	1.0	20	3days
9	Cyclic stress	PF+C	1.0	2.0	20	3days
10	Cyclic stress	PF+C	1.0	3.0	20	3days
11	Cyclic stress	Geofiber (A)	-	-	-	-
12	Cyclic stress	Geofiber (B)	-	-	-	-

13	Cyclic stress	Geofiber (C)	-	-	-	-
14	Cyclic strain	Sand	-	-	-	-
15	Cyclic strain	PF	1.0	-	20	-
16	Cyclic strain	PF	0.50	-	20	-
17	Cyclic strain	PF	1.0	-	10	-
18	Cyclic strain	PF	0.50	-	10	-
19	Cyclic strain	PF+C	1.0	1.0	20	3days
20	Cyclic strain	PF+C	1.0	2.0	20	3days

Note: CP: Confining Pressure, FC: Fiber Content, CC: Cement Content, FL: Fiber Length, D<sub>r</sub>: Relative Density.

### Formulation Used

As shown in Figure 6, the shear modulus is calculated as the slope of a secant line connecting the extreme points on a hysteresis loop at a given shear strain.

The slope of the secant line connecting the extreme points on the hysteresis loop is the Young's modulus (E), as determined by cyclic triaxial test results (Towhata 2008).

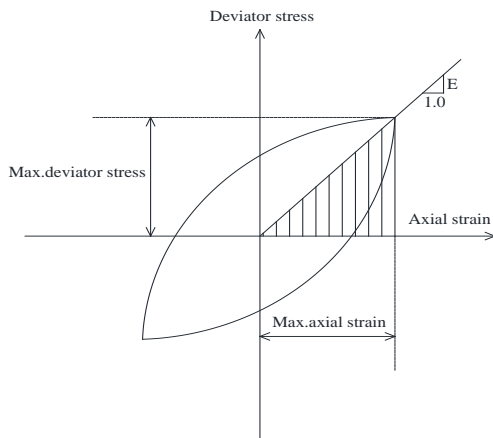


Figure (7): Hysteretic stress-strain relationship

$$\gamma = (1 + \mu)\epsilon \quad (1)$$

$$E = \frac{\sigma_{d \max}}{\epsilon_{\max}} \quad (2)$$

$$G = \frac{E}{2(1 + \mu)} \quad (3)$$

$$CSR = \frac{1}{2} * \left( \frac{\sigma_1' - \sigma_3'}{\sigma_3'} \right) \quad (4)$$

where  $\gamma$  is the shear strain,  $\mu$  is the Poisson's ratio which equals 0.50,  $\epsilon$  is the cyclic axial strain, E is young's modulus,  $\sigma_{d \max}$  is the maximum deviator stress,  $\epsilon_{\max}$  is the maximum axial strain, G is the shear modulus, CSR is the cyclic stress ratio,  $\sigma_1'$  and  $\sigma_3'$  are, respectively, the maximum and the minimum principal

effective stresses.

To aid in the evaluation of reinforcing efficiency, the liquefaction improvement factor (LIF) is defined as follows:

$$LIF = \left[ \frac{N_r - N_u}{N_u} \right] * 100 \quad (5)$$

where  $N_u$  and  $N_r$  are the number of load cycles required to cause liquefaction for unreinforced and reinforced specimens, respectively.

## TEST RESULTS AND DISCUSSION

Figures 8 (a)-(d) depict typical outcomes from a cyclic stress triaxial test on a reinforced specimen with a 30% initial relative density, 100 kPa initial effective confining pressure, 1% polypropylene fiber and 2% cement. As seen in the figure, when the accumulated excess pore water pressure equals the total stress under cyclic loading, the effective stress becomes zero (liquefaction state). The failure is defined as a full or 100 % pore pressure ratio ( $r_u = \frac{\Delta u}{\sigma'_0} = 1.0$ ).

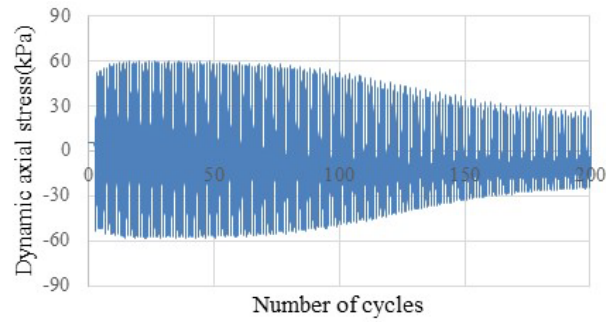
The influences of test parameters such as fiber properties, cement content and geofiber layers on liquefaction resistance and shear modulus are shown and discussed in the following sub-sections.

### Liquefaction Resistance

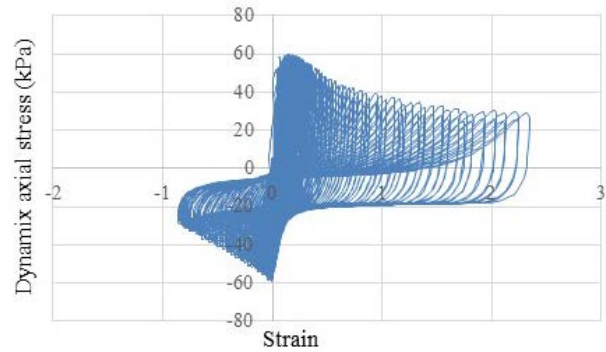
#### Shear Modulus

The shear modulus of unreinforced and reinforced sands is computed and explained in this sub-section. The variation in maximum shear modulus ( $G_{\max}$ ) as a function of fiber content percentage is seen in Figure 9.  $G_{\max}$  increases as fiber and cement contents increase, as indicated in the graph. At a shear strain of 0.03 %, the shear modulus is calculated using a cyclic strain-controlled triaxial test. Figure 8 shows  $G_{\max}$  values for plain sand and sand with polypropylene fibers, noting

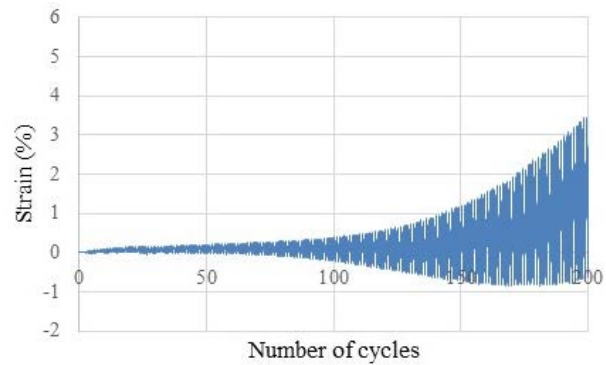
that these values are close to those reported by Noorzad and Fardad Amini (2014).



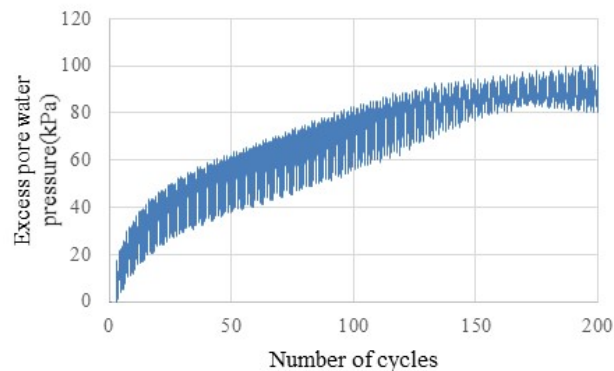
(a)



(b)



(c)



(d)

**Figure (8): Typical cyclic triaxial test results for specimen with  $D_r = 30\%$ ,  $FL = 20$  mm,  $CSR = 0.30$ , initial effective confining pressure = 100 kPa, 2% cement + 1% polypropylene fiber (a) dynamic axial stress versus number of load cycles (b) dynamic axial stress versus strain (c) strain versus number of load cycles and (d) excess pore water pressure versus number of load cycles**

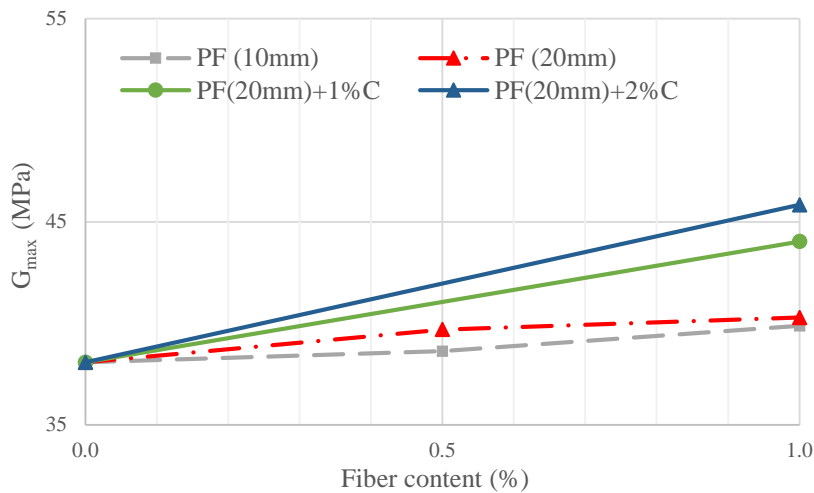


Figure (9):  $G_{max}$  vs. polypropylene fiber content ( $D_r=30\%$ , shear strain=0.03% and  $\sigma_0'=100$  kPa)

### Effect of Fiber Length

Figure 10 shows the influence of different cyclic stress ratios on the length of polypropylene fibers. The figure shows that polypropylene fiber with a length of 20mm outperforms polypropylene fiber with a length of 10mm at the same fiber content, demonstrating that fiber length is important in liquefaction resistance. At  $CSR = 0.20$ ,  $D_r=30\%$  and  $\sigma_0'=100$  kPa, the liquefaction improvement factor (LIF) of adding 1% PF of 20-mm length is equal to 215.38%. Figure 11 shows the influence of the length of polypropylene fiber on the generation of the excess pore water pressure with increasing the number of cycles. The increase in the length of polypropylene fiber at the same fiber content decreases the rate of generation of the excess pore water pressure, as shown in the figure.

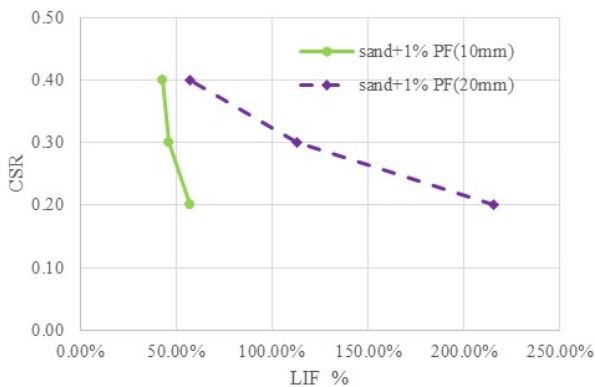


Figure (10): CSR vs. LIF (%) for different polypropylene fiber lengths ( $D_r=30\%$  and  $\sigma_0'=100$  kPa)

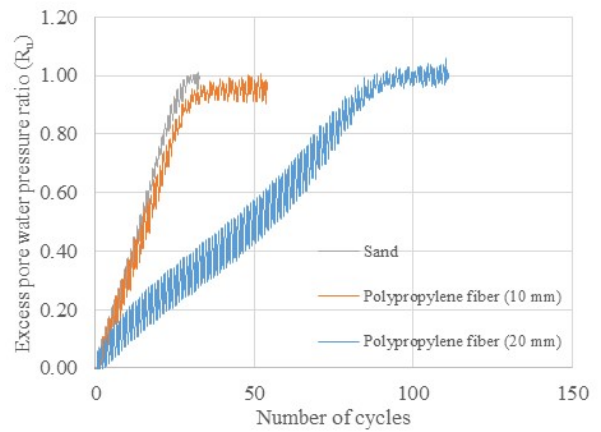
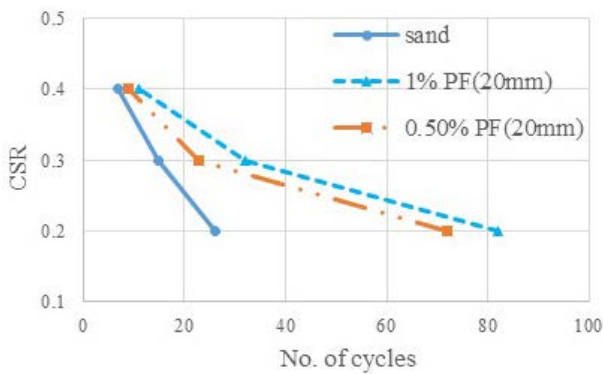


Figure (11): Excess pore water pressure ratio vs. number of cycles for different lengths of polypropylene fiber ( $D_r=30\%$ ,  $\sigma_0'=100$  kPa, F.C=1.0% and  $CSR=0.20$ )

### Effect of Fiber Content

The effect of fiber content on liquefaction resistance is depicted in Figure 12. Liquefaction resistance was higher with 1.0% polypropylene fibers compared with 0.50% polypropylene fibers. At  $CSR = 0.20$ ,  $D_r=30\%$  and  $\sigma_0'=100$  kPa, the liquefaction improvement factor (LIF) of adding 1.0% polypropylene fibers is equal to 1.22 times that in the case of addition of 0.50% of polypropylene fibers, indicating that fiber content has a significant impact on liquefaction resistance. Figure 13 shows the effect of fiber content on the shear modulus of the specimens. At different shear strains, as fiber content increases, the shear modulus also increases.



**Figure (12): CSR vs. number of cycles for different contents of polypropylene fiber ( $D_r=30\%$  and  $\sigma_0'=100\text{kPa}$ )**

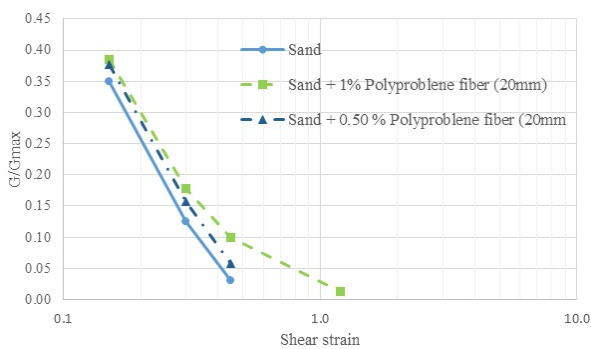


**Figure (13):  $G/G_{max}$  vs. shear strain for different contents of polypropylene fiber ( $D_r=30\%$  and  $\sigma_0'=100\text{kPa}$ )**

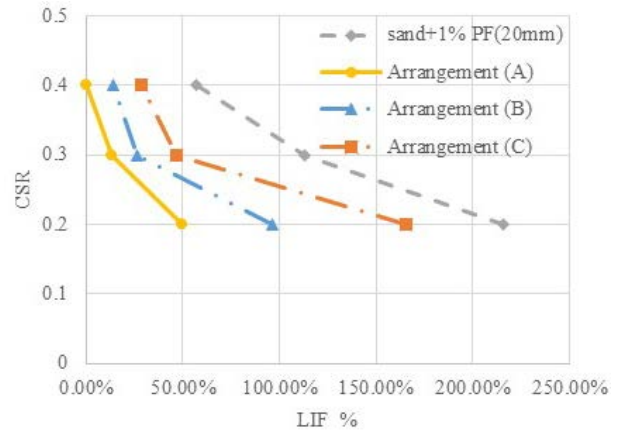
**Effect of Adding Geofibers**

Figure 14 shows the degree of enhancement of adding geofibers to sand specimens. The arrangement (C) of geofibers gave more liquefaction resistance than arrangements (A) and (B), so the addition of geofibers enhances the liquefaction resistance. The liquefaction improvement factor (LIF) of the addition of geofibers (arrangement C) is equal to 165% at  $CSR = 0.20$ ,  $D_r=30\%$  and  $\sigma_0'=100\text{ kPa}$ .

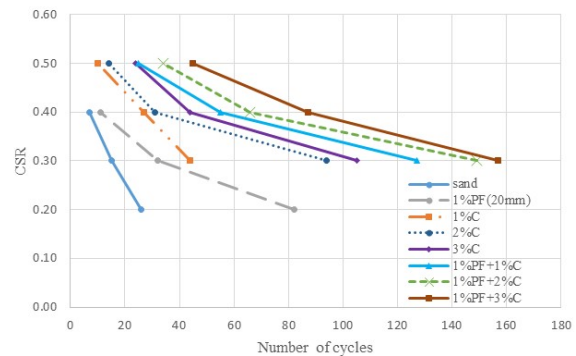
**Effects of Adding Cement and Cement with Polypropylene Fibers**

Figure 15 depicts the effects of adding cement to sand specimens and adding polypropylene fibers to cement. The addition of cement gave more cycles than the addition of polypropylene fibers alone. The presence of cement increases the strength and resistance of the liquefaction phenomenon and the addition of fibers to cement raises the strength and resistance even more because of the extra links formed between fibers and

sand. At  $CSR = 0.30$ ,  $D_r=30\%$  and  $CP=100\text{ kPa}$ , the liquefaction improvement factor (LIF) of adding 3.0% C + 1% PF is equal to 1.58 times that of the addition of 3.0% C, implying that adding fibers to cement improves liquefaction resistance significantly.



**Figure (14): CSR vs. LIF for different arrangements of geofibers ( $D_r=30\%$  and  $\sigma_0'=100\text{ kPa}$ )**



**Figure (15): CSR vs. number of cycles for specimens reinforced with cement and polypropylene fibers ( $D_r=30\%$  and  $\sigma_0' =100\text{ kPa}$ )**

**Comparison between Different Types of Additives**

Figure 16 illustrates the amounts of improving the strength and liquefaction resistance for the additives used in the present study. The addition of 3% C+1% PF gave the best liquefaction resistance compared with other additives. The liquefaction improvement factor (LIF) of specimens reinforced with 3% C+1% PF equals 946.67% at  $CSR=0.30$ ,  $D_r=30\%$  and  $\sigma_0' =100\text{ kPa}$ . As a result, cement and fiber reinforcement plays a major role in improving the liquefaction resistance.



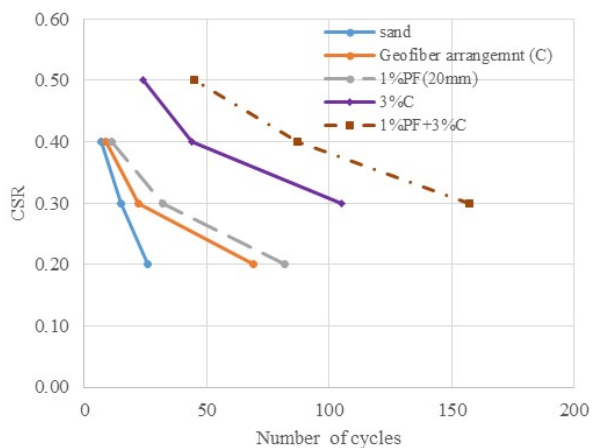


**Figure (16): CSR vs. number of cycles for specimens reinforced with different additives ( $D_r=30\%$  and  $\sigma'_0=100\text{kPa}$ )**

### CONCLUSIONS

The effect of several types of additives on the liquefaction behavior of sandy soil was evaluated using an experimental programme. On both unreinforced and reinforced sand, a series of cyclic stress triaxial tests and cyclic strain triaxial tests were conducted.

1. The liquefaction resistance of reinforced sand was controlled by fiber content, fiber length, geofiber arrangement and cement content. Increases in fiber

content, fiber length and cement content can all greatly reduce liquefaction.

2. The liquefaction improvement factor (LIF) increased when fiber length increased. The liquefaction improvement factor (LIF) of the addition of 1% PF of 20-mm length is equal to 215.38% at  $CSR = 0.20$ ,  $D_r=30\%$  and  $CP=100\text{ kPa}$ .
3. As fiber content increased, LIF increased. LIF of adding 1.0 % polypropylene fibers is equal to 1.22 times the addition of 0.50% of polypropylene fibers.
4. The addition of geofibers increased the liquefaction resistance as the number of layers increased. Arrangement (C) gave better liquefaction resistance than arrangements (A) and (B). The liquefaction improvement factor (LIF) of the addition of geofibers (arrangement C) is equal to 165% at  $CSR = 0.20$ ,  $D_r=30\%$  and  $CP=100\text{ kPa}$ .
5. The presence of cement increases the strength and resistance to the liquefaction phenomenon and the addition of fibers to cement raises the strength and resistance even more.

The addition of 3% C+1% F gave the best liquefaction resistance in this study. The liquefaction improvement factor (LIF) of specimens reinforced with 3% C+1% PF equals 946.67%, so reinforcement with cement and fibers plays an important role in improving the liquefaction resistance.

### REFERENCES

- Ahmad, F., Bateni, F., and Azmi, M. (2010). "Performance evaluation of silty sand reinforced with fibers." *Geotextiles and Geomembranes*, 28 (1), 93-99.
- Alhassani, A.M.J. (2021). "Improvement of sandy soil using materials of sustainable consideration." *Jordan Journal of Civil Engineering*, 15 (4), 623-632.
- Alibolandi, M., and Moayed, R.Z. (2015). "Liquefaction potential of reinforced silty sands." *International Journal of Civil Engineering*, 13 (3-4), 195-202.
- ASTM D3999/D3999M-11. (2013). "Standard test methods for the determination of the modulus and damping properties of soils using the cyclic triaxial apparatus".
- ASTM D5311/D5311M-13. (2013). "Standard test method for load controlled cyclic triaxial strength of soil (D5311-92)". Annual book of ASTM standards.
- Consoli, N.C., Vendruscolo, M.A., Fonini, A., and Rosa, F.D. (2009). "Fiber-reinforcement effects on sand considering a wide cementation range". *Geotextiles and Geomembranes*, 27 (3), 196-203.
- Ghadr, S., Samadzadeh, A., Bahadori, H., and Assadi-Langroudi, A. (2020). "Liquefaction resistance of fibre-reinforced silty sands under cyclic loading." *Geotextiles and Geomembranes*, Elsevier, Ltd., 48 (6), 812-827.
- Ishihara, K. (1993). "Liquefaction and flow failure during earthquakes." *Geotechnique*, 43 (3), 351-451.
- Kumar, S., Sahu, A. K., and Naval, S. (2021). "Study on the swelling behavior of clayey soil blended with geocell and jute fibre". *Civil Engineering Journal (Iran)*, 7 (8), 1327-1340.
- Ladd, R.S. (1978). "Preparing test specimens using under-compaction". *Geotechnical Testing Journal*, 1 (1), 16-23.

- Mirmohammad Sadeghi, M., and Hassan Beigi, F. (2014). "Dynamic behavior of reinforced clayey sand under cyclic loading". *Geotextiles and Geomembranes*, Elsevier, 42 (5), 56-572.
- Mittal, A., and Shukla, S. (2020). "Effect of geofiber reinforcement on strength, thickness and cost of low-volume rural roads." *Jordan Journal of Civil Engineering*, 14 (4), 587-597.
- Naeini, S. A., and Zakiyeh, E. (2014). "Effect of geotextile on the liquefaction behavior of sand in cyclic triaxial test". *Scientific Cooperation International Workshops on Engineering Branches*, Koc University, Istanbul, Turkey, (August 2014), 63-67.
- Noorzad, R., and Fardad Amini, P. (2014). "Liquefaction resistance of Babolsar sand reinforced with randomly distributed fibers under cyclic loading." *Soil Dynamics and Earthquake Engineering*, Elsevier, Ltd., 66, 281-292.
- Robinson, S., Brennan, A.J., Knappett, J.A., Wang, K., and Bengough, A.G. (2019). "Cyclic simple shear testing for assessing liquefaction mitigation by fibre reinforcement." *Earthquake Geotechnical Engineering for Protection and Development of Environment and Constructions- Proceedings of the 7<sup>th</sup> International Conference on Earthquake Geotechnical Engineering*, 2019, CRC Press/Balkema, 4728-4735.
- Safdar, M., Newson, T., Schmidt, C., Sato, K., Fujikawa, T., and Shah, F. (2020). "Effect of fiber and cement additives on the small-strain stiffness behavior of Toyoura sand". *Sustainability (Switzerland)*, 12 (24), 1-17.
- Tang, C., Shi, B., Gao, W., Chen, F., and Cai, Y. (2007). "Strength and mechanical behavior of short polypropylene fiber-reinforced and cement-stabilized clayey soil." *Geotextiles and Geomembranes*, 25 (3), 194-202.
- Towhata, I. (2008). "Springer series in geomechanics and geoen지니어ing: Geotechnical earthquake engineering".